Separability Between Valence and Conduction Bands in Transition Metal Clusters

EDOARDO APRÀ,[1] EMILY A. CARTER,[2] ALESSANDRO FORTUNELLI[3]

[1] *Theory, Modeling and Simulation, Environmental Molecular Sciences Laboratory, Pacific Northwest National Laboratory, P.O. Box 999, Richmond, Washington 99352*

[2] *Department of Chemistry and Biochemistry, University of California at Los Angeles, Box 951569, Los Angeles, California 90095-1569*

[3] *Molecular Modeling Laboratory, Istituto per i Processi Chimico-Fisici (IPCF) del C.N.R., via V. Alfieri 1, 56010, Ghezzano (PI), Italy*

ABSTRACT: Simplified theories of transition metal electronic structure have been postulated for many decades. We test one such approximation, namely separate treatments of d (valence) and s/p (conduction) electrons in transition metal clusters, within a density functional theory (DFT) formalism. Two different basic approaches are considered: (a) an independent-band approximation, in which the d- and s/p-bands interact only via the ρ-dependent components of the Kohn–Sham operator; and (b) a more realistic approximation, in which the lowest-energy d- and s/p-orbitals (separately derived) are allowed to interact through explicit off-diagonal coupling matrix elements. The results are presented for the energy differences among three structural forms (icosahedral, cuboctahedral, and truncated decahedral) of 13-atom Ni and Pt clusters. We demonstrate that an explicit decoupling of the d- and s/p-bands does not produce accurate results for the clusters considered, not even for nickel, i.e., the transition metal for which d–s/p mixing should be at its minimum. By contrast, allowing the lowest-energy orbitals of the two separate bands to interact improves the results considerably, and ensures a fair description of metal–metal bonding. This finding suggests that simplified models that exclude explicit d–s/p coupling should be employed with caution.   © 2004 Wiley Periodicals, Inc. Int J Quantum Chem 100: 277–287, 2004

Key words: structural energy differences; d–s hybridization; electronic structure; transition and noble metals; inter-band mixing

Introduction

The theoretical description of systems containing transition metals (TMs) presents well-known difficulties, associated with the presence of two different open shells: a "valence" d-shell, with localized character often important for chemical bonding [1], and a "conduction" s/p-shell, with substantially delocalized character that gives rise to conventional metallic bonding. These difficulties are at their maximum in finite species such as clusters, due to the presence of boundaries and asymmetries. An accurate treatment of intra- and inter-shell polarization and correlation effects in pure TM clusters has proved extremely difficult (a prototypical example is the Cr_2 molecule, see Ref. [2] for an overview and recent perspectives), so much so as to limit the application of rigorous post-Hartree–Fock methods. Density functional theory (DFT) represents a convenient and quite successful alternative, providing results that are usually in reasonable agreement with experimental data. Despite the simplifications inherent in DFT—which is cast in a form equivalent to an independent-electron approximation—and the rapid development in computer technology, DFT calculations on systems containing hundreds of TM atoms are still very demanding from a computational point of view. Over the years, this has prompted a search for simplified methods, which would allow one both to extend the range of applicability of the theoretical machinery and, most importantly, to develop models for qualitative prediction, interpretation, and deeper understanding of TM chemistry and physics.

One of the main simplification strategies attempts to disentangle the mixing of the "valence" and "conduction" bands [3–18]. This would drastically simplify the problem, by splitting it into two separate, and much more affordable, problems. To be specific, the separate treatment of the d- and s/p-bands would allow one, for example, to use different theoretical approaches for the description of each of them [3–5] (S. C. Watson, E. A. Carter, M. K. Walters, and P. A. Madden, unpublished observations) or to develop a fully convincing and accurate tight-binding treatment of TMs [19]. (The general validity of such a treatment is still debated, whereas it has been successfully developed, e.g., for carbon- and silicon-based compounds [20].

Conceptual understanding of TMs based on some sort of separation between d- and s/p-electrons can be found in the literature for many decades [3] up to the present day [18].

Early on [4, 5], interpolation schemes for overlapping s/p-conduction and d-valence bands in bulk metals were developed. The conduction band was described within a nearly free electron formalism (in analogy with the pseudopotential method developed for simple metals [21]), whereas the d-band was treated within a tight-binding scheme, and their coupling was parameterized. This analysis, which was very detailed and insightful, concentrated on the representation of the band structure. From these results and further analysis [6, 7], it appeared that it was possible to model the electronic structure of bulk transition and noble metals in terms of d-resonant states immersed in the conduction band continuum. This oriented the research toward the development of approximate schemes based on a formal separation between d- and s/p-bands, especially in view of the study of cohesive energies [8–10]. In these schemes, the total energy of bulk transition and noble metals was mainly determined by two parameters—the width and the center of gravity of the d-band—while the role of s/p–d hybridization on the energy of cohesion was included only in a parametric way as an indirect influence on the center of the d-band or on the effective d–d interaction (despite an early suggestion by Mott [22] on the possible importance of s/p–d interactions on the total energy of cohesion). Along these lines, Wills and Harrison [11] combined the nearly-free-electron theory of simple metals with low-order perturbation theory in the valence band–conduction band coupling, ending up with a separate description of the two bands, in which the d-orbital interactions were described by a tight-binding Hamiltonian, plus a coupling term that amounted to a rigid shift of the d-band. In the same spirit, Hausleitner and Hafner [12] derived effective inter-atomic pair interactions from a combined nearly-free-electron treatment of the s/p-electrons and a tight-binding treatment of the d-electrons, where explicit d—s/p coupling was neglected. Several investigators [13–17] constructed one-electron effective core potentials for TMs, which implicitly decouple the d- and s/p-bands, sometimes augmented [15] by a diffuse attractive projection operator to account for d-orbital relaxation. Recently, a tight-binding model for TM clusters was proposed [18] in which no cross-coupling terms connect the d- and s/p-orbitals.

Originally, the analysis was mainly concerned with bulk systems [3–12]. However, when consid-

ering structural energy differences and moving to finite systems, one finds that (a) structural differences are due to a subtle interplay of different effects, which are difficult to account for through simplified (although physically transparent and appealing) analyses; (b) many terms cancel in the bulk for reasons of symmetry, but are important in finite systems due to the presence of boundaries and imperfections, so that, for example, tight-binding parameters derived from a fit of bulk systems cannot be simply transferred to clusters [23]. These effects are at their maximum when considering structural differences in small-to-medium-size clusters, quantities that are of great interest for their importance in the field of nanotechnology.

This motivated the present work, in which we present a detailed analysis of DFT calculations on selected TM clusters, aimed at numerically testing and verifying the predictive capabilities of the d–s/p separation for these systems. Platinum and nickel, residing as they do at the end of the transition series, represent elements in which d–s/p mixing should be least important and where such separate-band models should be most applicable. However, platinum is a third-row metal, in which the strong relativistic stabilization of the atomic s-shell produces a substantial hybridization with the d-shell, whereas nickel is a first-row metal, in which the contraction of the d-orbitals along the series should place the valence band–conduction band coupling at its minimum. If a decoupled d–s/p model does not work for nickel clusters, it will be unlikely to work for any other TM cluster.

We take small 13-atom clusters as test cases, Pt_{13} and Ni_{13} (Pt_2 is also treated as an introductory example), and concentrate on structural properties, i.e., on the reproduction of the energy differences among various highly symmetrical structural forms: icosahedral, cuboctahedral, and truncated decahedral [24–26]. This represents a stringent test of the capability of the d–s/p separation model to predict accurately the energetics of systems involving neutral TMs. Such energy differences are, in fact, extremely sensitive to the quality of the theoretical method, as well as being crucial for the prediction of the structural properties of nanoclusters (which, in turn, determine their properties, including optical, catalytic, and magnetic [27]). We defer an analysis of the effects of d–s/p interactions on more complex properties (e.g., elastic constants, dipole moments) and the development of specifically tailored approaches for their accurate prediction to further work.

This article is organized as follows. Section 2 provides calculational details; section 3 describes the theoretical strategy; section 4 presents results for Pt_2, Pt_{13}, and Ni_{13}; and section 5 summarizes our main conclusions.

2. Calculational Details

All calculations were carried out with the DFT module of the NWChem computational chemistry package (Release 4.1) [28], which uses Gaussian-type orbitals (GTO) for the solution of the Kohn–Sham equations. This module was purposely modified as explained in detail in the next section. The use of a GTO basis set allows us to distinguish unequivocally among the various local atomic symmetries.

For platinum, an effective core potential (ECP) [29] was used to represent the nucleus plus inner-shell (up to the $4f$ shell) core electrons interactions with all valence electrons; thus, only the outer-core ($5s$ and $5p$ shells) plus valence electron wave function is solved for explicitly. This ECP incorporates spin-orbit-averaged relativistic effects. The outer-core plus valence electrons were described using a $(7s5p5d)/[6s3p2d]$ atomic orbital basis, derived from a $(7s6p5d)/[6s3p2d]$ basis set [30] by removing the most diffuse p-function that causes numerical instabilities in these highly condensed systems, and splitting the first p-contraction of 4 GTO into 3 and 1 GTO. This basis set is of double-ζ quality for the d-set, but it accurately reproduces the results of a triple-ζ-plus-polarization basis set [30], as shown in Ref. [26]. For nickel, an all-electron $(17s11p6d)/[6s4p3d]$ atomic orbital basis was used, corresponding to the triple-ζ-plus-polarization basis set of Ref. [30].

All the calculations were performed spin-unrestricted, using the Becke functional [31] for exchange and the Perdew–Wang functional [32] for correlation, hereafter referred to as BPW91. We always found spin symmetry breaking for the systems considered in the present study; there was always an uneven number of α- and β-electrons for the ground-state wave functions.

A numerical integration is necessary for the evaluation of the exchange-correlation potential and energy. The scheme used in this work adopts well-known techniques that partition the density into atomic contributions [33]. This "atomic density" is then integrated using a radial quadrature [34] and a

TABLE I

Values (Å) of geometric parameters for Pt and Ni clusters optimized through the full DFT/BPW91 approach.*

Pt_2	O_hPt_{13}	I_hPt_{13}	$D_{5h}Pt_{13}$	O_hNi_{13}	I_hNi_{13}	$D_{5h}Ni_{13}$
2.380	2.725	2.682	2.914, 2.678 (0.462)	2.360	2.320	2.417, 2.341 (0.479)

* For 13-atom clusters, the distances of the peripheral atoms from the central one are reported. The truncated decahedral structure (D_{5h}) has a further degree of freedom, i.e., the ratio between the absolute value of the z-coordinates of the off-C_5 atoms and the apex atom (z is the C_5 axis); this ratio is shown in parentheses.

highly efficient angular quadrature [35], as explained in detail in Ref. [26].

To overcome the degeneracy problems that arise in systems such as these, containing many zero-valent TM atoms, a Gaussian smearing technique for the fractional occupation of the energy levels was applied [36, 37]. Smearing the one-electron levels is very beneficial, if not strictly necessary, to obtain smooth convergence for such quasi-metallic systems that have many extremely closely spaced energy levels [26]; smearing also prevents symmetry breaking in Jahn–Teller systems (i.e., with a degenerate, incompletely occupied highest-occupied molecular orbital [HOMO]). However, we checked that our results are not significantly affected by the use of the smearing technique. All the results reported below have been obtained using a smearing width: $\sigma = 0.0003$ Hartree.

3. Method

First, the geometries of the clusters were optimized using the full DFT/BPW91 method within the proper symmetry group: $D_{\infty h}$ (Pt_2), O_h (cuboctahedron), I_h (icosahedron), and D_{5h} (truncated decahedron). The optimized geometries are collected in Table I. Some of these results have been taken from previous work: for Pt_2, see Ref. [38]; for Pt_{13}, see Ref. [26]. The geometries of the clusters were fixed at their optimum (DFT/BPW91) values, and the converged full Kohn–Sham operator and overlap matrices (say, F and S) were extracted. Various procedures to disentangle d–s/p mixing have then been implemented, using an approach analogous to that developed in Ref. [19].

The simplest form of d–s/p separation would be to annihilate all the off-diagonal matrix elements of the F- and S-operators between d- and s/p-basis functions. However, this simplistic strategy is not feasible because of the presence of core (Ni) or

outer-core (Pt) functions, to which the d- and s/p-functions must be orthogonal.

In the first procedure we implemented (procedure A), we therefore defined a d-basis set and an s/p-basis set, separately Schmidt-orthogonalized the two basis sets to the core (Ni) or outer-core (Pt) functions, and diagonalized the Kohn–Sham operator (taking overlap into account) over the two separate spaces. Finally, we determined a new density matrix by an aufbau-occupation of the total (merged) spectrum, and evaluated the corresponding energy. This procedure corresponds to a sort of independent-band approximation, in which the bands interact via the ρ-dependent components of the Kohn–Sham operator, but they do not mix. In principle, the Kohn–Sham operator might be determined self-consistently. However, in the examples considered below, it usually proved impossible to reach convergence: the iterative process ended up either oscillating between two different states, or even diverging, despite the use of various numerical techniques to improve the convergence of the iterative process, so that the converged full Kohn–Sham operator has always been used in our analysis. We believe, however, that the results so obtained are representative of the "best" possible separate-band approximation.

A first step going beyond complete d–s/p separation can be achieved by reintroducing a partial coupling between the bands by allowing interaction among the lowest-energy d- and s/p-levels. An analysis of the separate d-, s-, and p-spectra obtained through procedure A showed us, in fact, that the one-electron eigenvalues are typically distributed into well-separated groups of levels of appropriate number (corresponding to the number of atoms multiplied by 1 for s-, 3 for p-, and 5 for d-functions). One can thus reintroduce s/p–d coupling at a minimal level either by allowing 5 orbitals per atom per spin symmetry in the d-spectrum and 1 orbital per atom per spin symmetry in the

s/p-spectrum to interact among themselves (procedure B), or by further separating the conduction space into an s- and a p-component, performing a separate diagonalization within the d-, s-, and p-basis sets properly Schmidt-orthogonalized to the core (Ni) or outer-core (Pt) functions, and finally allowing 5 orbitals per atom per spin symmetry from the d-spectrum, 1 orbital per atom per spin symmetry from the s-spectrum, and 3 orbitals per atom per spin symmetry from the p-spectrum to interact among themselves (procedure C). Recall that the residual function space not included in procedure C with respect to the full DFT approach amounts to $(2s1p2d)$ basis functions per atom for Ni_{13} and $(4s1p1d)$ basis functions per atom for Pt_{13}, respectively.

These three approximate procedures have been implemented within NWChem. The results on the test systems are presented in the next section.

Before entering into the analysis of the results, a technical remark is in order concerning the issue of s/p–d orthogonalization versus interaction. Historically, the main difference between the analysis in Refs. [4] and [5], in fact, consisted of the requirement imposed in the latter approach of explicit orthogonalization of the conduction band functions to the d-functions. We thus performed several calculations to check the separate importance of overlap and Kohn–Sham matrix elements. In detail, procedure A as outlined above consists in deriving separate d- and s/p-bands, determining which orbitals should be occupied via the aufbau principle in the merged spectrum, orthogonalizing the selected orbitals among themselves (e.g., through a Lowdin or a Schmidt orthogonalization), and finally evaluating the density and the energy accordingly. Alternatively, one can think of introducing orthogonalization before deriving separate d- and s/p-bands through the diagonalization procedure and finally determining which orbitals should be occupied via the aufbau principle in the merged spectrum. For example, as a preliminary step, one can explicitly Schmidt-orthogonalize the s/p-orbitals to the d-orbitals, or perform a Lowdin symmetrical orthogonalization of the two sets [5], before calculating the matrix elements of the Kohn–Sham operator over the two separate spaces. Or one can think of deriving the s/p-spectrum in a space orthogonal to the lowest-energy eigenvectors of the d-band (a sort of OPW approach). We tried all such possibilities, but found results very similar to those obtained through procedure A; therefore, the corresponding results will not be reported in the next section. Simple orthogonalization does not qualitatively modify the results; the reason is that the diagonal elements are not changed up to second order by the orthogonalization procedure [39].

Analogously, orthogonalization of the s/p- and d-bands to the core was not found to be an issue. We found in fact that (a) preliminary Schmidt orthogonalization to the core orbitals is essential to avoid variational collapse of the atomic-like basis set onto the core functions, but also that (b) this is sufficient to ensure that the mixed core-valence matrix elements of the Kohn–Sham operator after the orthogonalization are negligible. In other words, an "augmented conduction and valence functions" approach works for late TMs.

In passing, we note that spin-orbit (which is important for very heavy metals) can easily be dealt with within the present methodology.

4. Results and Discussion

PT_2

The one-electron spectrum of Pt_2 is schematically depicted in Figure 1a. The d-band gives rise to 5 bonding ($1\sigma_g$, π_u, δ_g) and 5 anti-bonding (δ_u, π_g, $1\sigma_u$) lowest-energy orbitals. For the s/p-band, only the lowest bonding ($2\sigma_g$) and anti-bonding ($2\sigma_u$) orbitals are shown. Fixing the inter-nuclear distance at the value optimized using the full DFT/BPW91 approach ($R = 2.380\ Å$), we applied the procedure prescribing a complete separation of the two bands (procedure A with the converged full Kohn–Sham operator), and compared the resulting energy and one-electron spectrum with the full DFT results in Table II. Note that α and β spin-orbital levels are reported, as we performed unrestricted calculations.

Several points can be made from an analysis of Table II. First, the electronic configuration obtained through the complete disentanglement of the two bands differs from the one derived form full DFT. At the most approximate level (procedure A) one obtains a configuration, $1\sigma_g^{1/1}\pi_u^{2/2}\delta_g^{2/2}2\sigma_g^{1/1}\delta_u^{2/2}\pi_g^{2/1}1\sigma_u^{1/0}$, instead of the $1\sigma_g^{1/1}\pi_u^{2/2}\delta_g^{2/2}2\sigma_g^{1/1}\delta_u^{2/2}\pi_g^{2/0}1\sigma_u^{1/1}$ full DFT configuration (the superscripts define the number of α/β electrons for each molecular orbital). This is because the occupied $1\sigma_u$ (d) orbital is stabilized through the interaction with the lowest virtual $2\sigma_u$ (s/p) orbital, and drops below the π_g (d) orbitals [38]. This is the simplest example of a switch in the one-electron energy ordering,

(a) Pt$_2$

s/p-band   d-band

(b) Pt$_n$

s/p-band   d-band
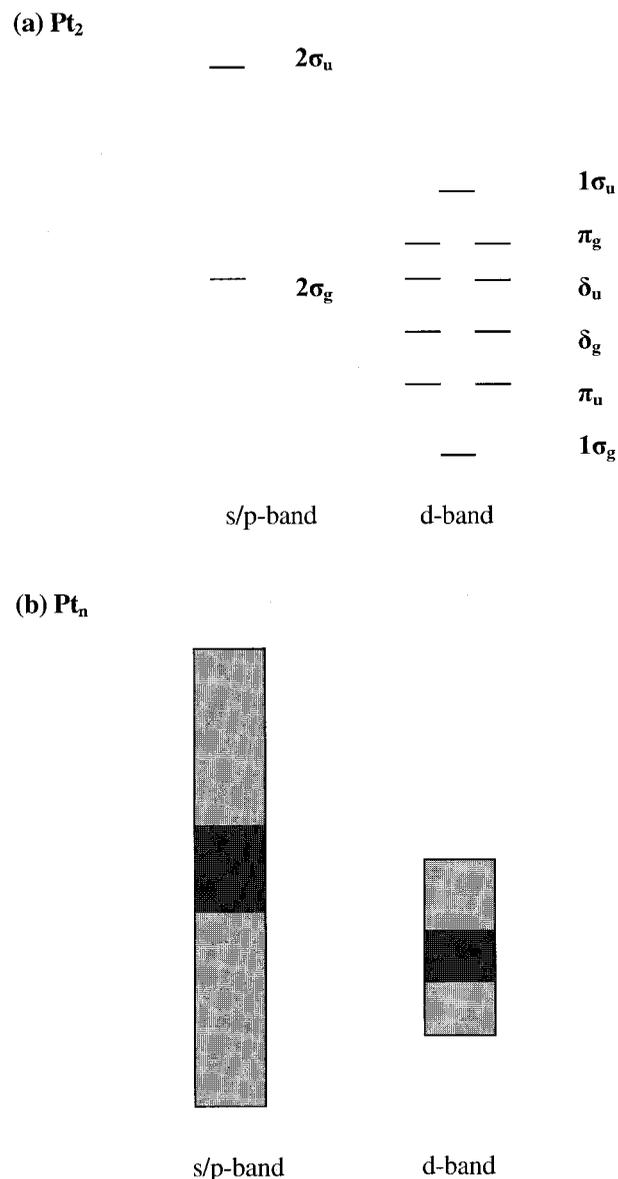
FIGURE 1. Schematic one-electron energy levels for (a) Pt$_2$ and (b) an extended Pt$_n$ condensed-phase system (the darker shade of gray represents regions with a higher density of states).

which is to be expected when neglecting d–s/p interactions.

Second, the binding energy (BE) is decreased by a factor of ~2/3 in the most approximate approach. A detailed analysis of the one-electron energy differences shows that there is no large discrepancy between the approximate and full DFT results. Rather, it is the sum of several small (≤ 0.1 eV, except for the $1\sigma_u$ orbital) all-positive contributions

that makes up such a large total energy difference (no error cancellation). The values of one-electron energies for $1\sigma_g$ and $2\sigma_g$ orbitals are those obtained after allowing for their mutual interaction (the total energy is invariant with respect to such linear combinations). The corresponding values before allowing for their interaction are: $-8.77/-8.40$ eV and $-7.20/-6.95$ eV for α/β spin-orbitals, respectively.

The inaccurate description of the bonding using procedure A also reflects on other quantities. As an example, when we relaxed the constraint of a fixed internuclear distance and we tried to optimize it, the optimized value using procedure A came out to be 2.51 § instead of 2.38 Å, with a gain in binding energy of 0.11 eV.

Given this situation, trying to derive a self-consistent solution proved impossible: an attempt in this direction produced a wildly diverging or a bimodal oscillating iterative process (this also applies to Pt$_{13}$ and Ni$_{13}$).

One may try to enforce the correct electronic configuration by an ad hoc switch of the π_g and σ_u orbitals, but the binding energy deteriorates to 1.75 eV instead of 2.10 eV (see Table II). In other words, the aufbau principle still holds for the approximate procedures. This is true in general: we have applied this procedure also to Pt$_{13}$ and Ni$_{13}$, always obtaining consistently worse results, so we do not report them for the larger clusters.

It is also not a problem connected with orthogonality effects. We have tried, in fact, to derive the s/p-spectrum in a space orthogonal to the occupied d-band, or to orthogonalize the s/p- and d-bands prior to their merging, as anticipated in section 3, but we do not find significant differences. This is reasonable, as the d–s/p overlaps in the absence of constraints do not exceed 0.14 in absolute value, which is a reasonable value for the localization procedure to make sense [39].

In contrast, by readmitting some sort of d–s/p interaction (procedures B and C), the results improve, as shown in Table II. Both procedures reduce the error in the total energy (yielding BE = 2.24–2.48 eV), give reasonable values of one-electron energy levels, and predict the correct electronic configuration. However, when we relaxed the constraint of a fixed inter-atomic distance, we still found an inaccurate results for the optimized value: $R_{\text{opt}} = 2.47$ Å from procedure C.

One can conclude that d–s/p coupling is essential for an accurate description of bonding in Pt$_2$, and that its complete neglect (procedure A) produces

TABLE II

Binding energy (BE), difference in the number of α and β electrons (N_α–N_β) and α/β one-electron occupied energy levels for Pt_2 calculated according to the methods described in the test.[*]

	A	B	C	Full DFT
BE	2.10	2.24	2.48	3.27
N_α–N_β	2	2	2	2
$1\sigma_g$	−9.52/−9.08	−9.52/−9.08	−9.52/−9.09	−9.64/−9.22
π_u	−8.36/−7.38	−8.36/−7.38	−8.37/−7.40	−8.37/−7.40
δ_g	−6.34/−5.94	−6.34/−5.94	−6.34/−5.94	−6.34/−5.94
$2\sigma_g$	−6.21/−6.04	−6.21/−6.04	−6.23/−6.07	−6.31/−6.14
δ_u	−5.81/−5.39	−5.81/−5.39	−5.81/−5.39	−5.81/−5.39
π_g	−6.14/−5.01	−6.14/−	−6.16/−	−6.16/−
$1\sigma_u$	−5.33/−	−5.42/−5.14	−5.47/−5.18	−5.66/−5.37

* Full DFT/BPW91 approach and procedures A, B, and C. The geometry is that optimized through the full DFT/BPW91 approach, $R = 2.380$ Å. Energy levels are replaced by a hyphen (-) when the corresponding orbitals are not occupied (note that the electronic configuration according to procedure A is $\cdots \pi_g^{2/1}$, so that the π_g orbitals contain only one electron in the β spin symmetry). Energies are expressed in eV.

substantial errors, whereas procedures B and C start accounting for such a coupling.

Let us now see whether this holds also for the larger clusters.

PT_{13}

The results of DFT calculations on the Pt_{13} cluster in various structural arrangements according to the procedures described in section 3 are reported in Table III. The geometries are those optimized at the full DFT/BPW91 level, and the various approximate procedures are implemented using the converged full Kohn–Sham operator. The icosahedral, cuboctahedral, and truncated decahedral structures, displayed in Figure 2, are the most likely candidates for lowest-energy configurations among the highly symmetrical ones, and from the subtle interplay of their energy ordering much can be said about the preferred geometries of metal nanoclusters [24–26]. For platinum, the truncated decahedral structure (D_{5h}) turns out to be the lowest-energy one, while the icosahedral structure is the least stable (even though by allowing symmetry breaking one finds other, less symmetrical, configurations lying below the truncated decahedral one [26]). The first point to emphasize from an analysis of Table III is that the complete decoupling of the s/p- and d-bands (procedure A) gives extremely poor values of binding energy per atom (BE/N) and completely alters the ordering of the structural arrangements by favoring the cuboctahedral (O_h)

TABLE III

Results of DFT calculations on Pt_{13} and Ni_{13} clusters according to the procedures explained in the text.[*]

	A		B		C		Full DFT	
	BE/N	N_α–N_β	BE/N	N_α–N_β	BE/N	N_α–N_β	BE/N	N_α–N_β
$I_h Pt_{13}$	−0.158	14	2.258	8	2.447	8	3.144	8
$O_h Pt_{13}$	0.766	14	2.320	6	2.510	6	3.182	6
$D_{5h} Pt_{13}$	0.168	8	2.305	4	2.537	4	3.216	4
$O_h Ni_{13}$	0.585	14	2.097	6	2.798	6	3.147	6
$D_{5h} Ni_{13}$	−0.301	20	2.103	8	2.835	8	3.182	8
$I_h Ni_{13}$	0.650	20	2.084	8	2.867	8	3.231	8

* The geometries of the clusters are those optimized through the full DFT/BPW91 approach, and the various approximate procedures are implemented using the converged full Kohn–Sham operator. BE/N (eV) is the binding energy per atom, N_α–N_β is the difference in the number of α and β electrons.

I_h

D_{5h}

O_h
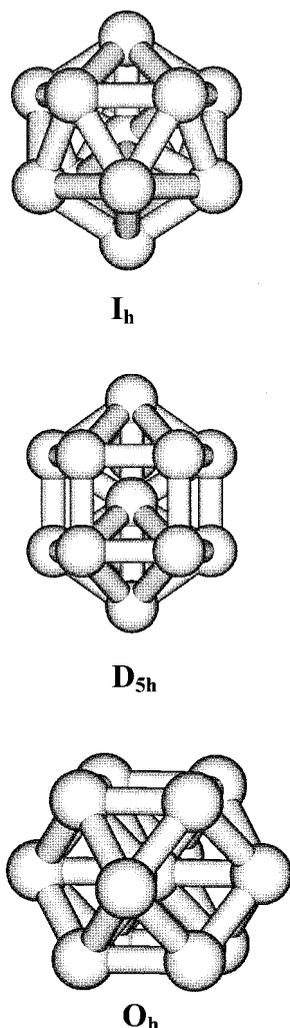
FIGURE 2. Schematic structures of the 13-atom clusters considered in the present work.

one by ~8 eV, which thus becomes the lowest in energy. All the subtleties of the metallic bonding as a function of the structural form are thus lost, spoiling the predictive capabilities of the approach. A clear sign of this can be seen in the difference in the number of majority (α) and minority (β) electrons: one gets roughly doubled values of this quantity through procedure A.

This can be explained in terms of the energy diagram reported in Figure 1b. The center of gravity of the d-band lies below that of the s/p-band (the corresponding energy difference is typically ≈ 1 eV for these clusters). However, the s/p intra-band splittings are larger than the d-ones (due to the more extended, delocalized character of the former), so that some of the s/p-levels lie below

some of the d-levels. If one neglects their mutual interaction, one misses their "repulsion" and therefore the destabilization of some of the d-levels close to the Fermi energy (nonbonding), with disastrous consequences on the total energy value. It should be stressed that this interaction is very selective (involving specifically the orbitals of the most interacting symmetries, such as a_{1g} and t_{2g} for the cuboctahedral O_h structure, with 1–1.5 eV as a typical range for the value of destabilization energy), and cannot be approximated as a uniform rigid shift of the d-band, as in earlier approximations [11, 12].

Moreover, small-to-medium-size TM clusters typically exhibit spin symmetry breaking; this holds for platinum, which is a nonmagnetic metal in the bulk, and a fortiori for nickel. In such systems, the α-band is stabilized by the exchange interaction with respect to the β-band, so that the center of gravity of the former is shifted downwards with respect to that of the latter. When the s/p "repulsion" is neglected, some of the unoccupied d-levels will be incorrectly stabilized, and will drop below the Fermi energy, thus becoming occupied. To accommodate these newly stabilized d-levels, other d-levels become depleted at the Fermi level. For TMs at the end of the transition series, the β density of states is larger than the α one (the darker area in Fig. 1b) and therefore β-spin electrons near the Fermi level are preferentially depleted. The excess of spin thus will be predicted to be larger than when allowing the d- and s/p-bands to interact. Enforcing the correct one-electron level ordering and electronic configuration, furthermore, is not beneficial (as in the Pt_2 case) because one still misses the stabilizing changes in the form of the orbitals associated with inter-band mixing: to be specific, the binding energy further deteriorates and assumes negative values for all the structures considered here.

The reintroduction to some extent of d–s/p coupling, instead, produces reasonable results. Procedure C in particular is capable of fairly predicting the energy differences among the structural forms, and the correct excess of spin, despite the fact that there is still a substantial error on the BE/N value: ~0.68 eV. By contrast, while procedure B obtains the correct spin states, it still does not quite recover the correct ordering of structures. The difference between procedures B and C lies in the number of spin-orbitals (1 vs. 4, per atom, per spin symmetry) in the s/p-band allowed to mix with the d-band spin-orbitals. It appears that the extra variational degrees of freedom associated with the p-orbitals

are critical for structural predictions. This is consistent with the fact that the p-orbitals will describe angular components to metal–metal bonding not captured by the s-band alone. Such angular metal–metal bonding appears to be important to predict cluster structural energy differences accurately.

We also checked that the electronic configuration is approximately reproduced when using procedure C. However, we still found differences close to the Fermi level; for example, in the spectrum of O_h Pt_{13}, the t_{2u} and e_g β spin-orbitals [26, 40] become fully occupied in procedure C, with a flow of electrons from the highest occupied t_{1u} to these and the lowest unoccupied t_{1g} spin-orbitals (analogous differences were found for D_{5h} and I_h Pt_{13}).

NI_{13}

The results of DFT calculations on the various structural forms of Ni_{13} according to the procedures described in section 3 are reported in Table III. With respect to Pt_{13}, one finds a similar value of BE/N, but a completely different energy ordering in which the icosahedral structure is now the lowest-energy one. This was expected on the basis of the reduced contribution of the d-orbitals to the bonding [24, 25]. Despite this, the complete separation of the valence and conduction bands again gives poor results. The relative energy of the cuboctahedral and icosahedral structures is in the correct range, but the truncated decahedral structure is destabilized by $\sim$12 eV, thus missing completely this structural form in the energy sequence. This shows how error cancellation may occasionally produce reasonable results for relative energies, e.g., binding energies, but this is not to be expected in the general case. The grossly overestimated values of the excess of spin from procedure A confirm the poverty of the description obtained through d–s/p separation and are in agreement with the analysis given in the previous subsection: the d–s/p interaction is essential in determining the correct energy order of the one-electron levels.

Here again, accounting for inter-shell interactions (procedure C) dramatically improves the results, by consistently bringing the error in BE/N values to $\sim$0.35 eV for all three structures and by predicting the correct value of the spin symmetry breaking (see Table III). The residual error in the BE/N value of $\sim$0.35 eV is about one-half that found for Pt_{13} ($\sim$0.68 eV), which confirms the lesser extent of d–s/p mixing for the first-row TM. In contrast, procedure B performs less well for Ni_{13}

than for Pt_{13}, confirming the lesser influence of p-functions for Pt, due to the relativistic stabilization of the atomic s-shell [19], as well as demonstrating again the sensitivity of structural energy differences to angular metal–metal bonding contributions.

We have checked that in this case the electronic configurations also stay the same as in the full DFT calculation when using procedure C (small differences are found when using procedure B). On the contrary, we found that procedure A predicts a consistent artificial flow of $\sim$10–12 electrons among the various orbital symmetries from the s/p-band to the d-band: the one-to-one correspondence between symmetry spin-orbitals with the full DFT calculation is more recognizable than in the Pt case, but still far from accurate.

Even though further work is required to check the fair results of procedure C more thoroughly, this procedure appears to be a good candidate for developing an approximate yet physically accurate description of TMs (see the developments in ref. [19]).

5. Conclusions

We have investigated the possibility of a simplified treatment of TM clusters through uncoupling of the valence (d)- and conduction (s/p)-bands.

The main conclusions drawn from the present analysis can be summarized as follows:

1. A complete decoupling of the two bands does not produce an accurate description of the electronic structure and energetics of TM clusters, in contrast to many simplified models that have assumed this decoupling in the past. This coupling is in fact responsible for a substantial fraction of the metal–metal bonding and for the subtle differences among the various structural forms for the clusters considered here.

2. The effect of d–s/p hybridization on the total energy cannot be approximated as a uniform shift of the d-band: the structural energy differences in clusters are precisely dependent on the detailed position of the d- and s/p-levels (due to self-consistent effects, etc.) and cannot be treated as a resonance between localized d-states immersed in a continuum of conduction states.

3. The orbitals belonging to the least-degenerate representations are the most interacting and selectively interacting, with levels strongly pushed up, etc.

4. A connection exists between accurate reproduction of the one-electron energy level spectrum and the total energy, which precludes cancellation of errors.

5. For spin-broken systems, as most small-to-medium-size clusters are (even of nonmagnetic metals), a further complication arises connected with the preferential depletion of spin states at the Fermi level.

6. The discrepancy between approximate and full DFT treatments does not decrease going from Pt_2 to Pt_{13}, i.e., with increasing size. Therefore, one should not expect improved results for extended systems (bulk, surfaces), in agreement with evidence that d–s/p mixing is relevant also for these systems [41].

7. Comparison between platinum and nickel shows that the degree of inter-band mixing varies from metal to metal. However, it is still not negligible for nickel, i.e., the TM in which this effect should be at its minimum.

8. Separate band diagonalization gives rise to spectra in which the one-electron eigenvalues are typically distributed into well-separated groups of levels of appropriate number: modified procedures which reintroduce an interaction among the lowest-energy groups of d- and s/p-levels account for a sizeable part of the inter-band mixing and correctly predict structural energy differences. This is similar in spirit to what is done in tight-binding treatment of TMs [19, 20]. The use of a properly parametrized tight-binding scheme is therefore supported by the present analysis, subject to the condition that the issue of the transferability of the tight-binding parameters among different molecular orbitals can be solved. In any case, such treatment should be more accurate for nickel than for platinum.

References

1. Taylor, S.; Lemire, G. W.; Hamrick, Y. M.; Fu, Z.; Morse, M. D. J Chem Phys 1988, 89, 5517.

2. Thomas, E. J. III; Murray, J. S.; O'Connor, C. J.; Politzer, P. J Mol Struct (Theochem) 1999, 487, 177.

3. Ziman, J. M., Ed. The Physics of Metals, Vol. 1: Electrons; Cambridge University Press: Cambridge, 1969.

4. Hodges, L.; Ehrenreich, H.; Lang, N. D. Phys Rev 1966, 152, 505.

5. Mueller, F. M. Phys Rev 1967, 153, 659.

6. Heine, V. Phys Rev 1967, 153, 673.

7. Phillips, J. C.; Mueller, F. M. Phys Rev 1967, 155, 594.

8. Watson, R. E.; Ehrenreich, H.; Hodges, L. Phys Rev Lett 1970, 24, 829.

9. Hodges, L.; Watson, R. E.; Ehrenreich, H. Phys Rev B: Condens Matter 1972, 5, 3953.

10. Gelatt, C. D., Jr.; Ehrenreich, H.; Watson, R. E. Phys Rev B: Condens Matter 1977, 15, 1613.

11. Wills, J. M.; Harrison, W. A. Phys Rev B: Condens Matter 1983, 28, 4363.

12. Hausleitner, C.; Hafner, J. J Phys: Condens Matter 1989, 1, 5243.

13. Melius, C. F.; Olafson, B. D.; Goddard, W. A., III, Chem Phys Lett 1974, 28, 457.

14. Hay, P. J.; Martin, R. L. J Chem Phys 1985, 83, 5174.

15. Panas, I.; Siegbahn, P.; Wahlgren, U. Chem Phys 1987, 112, 325.

16. Zurita, S.; Rubio, J.; Illas, F.; Barthelat, J. C. J Chem Phys 1996, 104, 8500.

17. Salazar, M. R.; Kress, J. D.; Redondo, A. Surf Sci 2000, 469, 80.

18. Berthier, G.; Defranceschi, M.; Montagnani, R.; Salvetti, O. Int J Quantum Chem 2001, 82, 26.

19. Fortunelli, A.; Velasco, A. M. Int J Quantum Chem 2004, 99, 654.

20. Goringe, C. M.; Bowler, D. R.; Hernandez, E. Rep Prog Phys 1997, 60, 1447.

21. Harrison, W. A. Phys Rev 1960, 118, 1182.

22. Mott, N. F. Adv Phys 1964, 12, 325.

23. Mercer, J. L.; Chou, M. Y. Phys Rev B: Condens Matter 1994, 49, 8506.

24. Cleveland, C. L.; Landman, U.; Schaaff, T. G.; Shafigullin, M. N.; Stephens, P. W.; Whetten, R. L. Phys Rev Lett 1997, 79, 1873; Häkkinen, H.; Moseler, M.; Landman, U. Phys Rev Lett 2002, 89, 033401.

25. Baletto, F.; Ferrando, R.; Fortunelli, A.; Montalenti, F.; Mottet, C. J Chem Phys 2002, 106, 3856.

26. Aprà, E.; Fortunelli, A. J Phys Chem A 2003, 107, 2934.

27. Klabunde, K. J. Nanoscale Materials in Chemistry; Wiley: New York, 2001.

28. Harrison, R. J.; Nichols, J. A.; Straatsma, T. P.; Dupuis, M.; Bylaska, E. J.; Fann, G. I.; Windus, T. L.; Aprá, E.; Anchell, J.; Bernholdt, D.; Borowski, P.; Clark, T.; Clerc, D.; Dachsel, H.; de Jong, B.; Deegan, M.; Dyall, K.; Elwood, D.; Fruchtl, H.; Glendening, E.; Gutowski, M.; Hess, A.; Jaffe, J.; Johnson, B.; Ju, J.; Kendall, R.; Kobayashi, R.; Kutteh, R.; Lin, Z.; Littlefield, R.; Long, X.; Meng, B.; Nieplocha, J.; Niu, S.; Rosing, M.; Sandrone, G.; Stave, M.; Taylor, H.; Thomas, G.; van Lenthe, J.; Wolinski, K.; Wong, A.; Zhang, Z. NWChem, A Computational Chemistry Package for Parallel Computers, Version 4.1; Pacific Northwest National Laboratory: Richland, WA, 2002.

29. Andrae, D.; Haeussermann, U.; Dolg, M.; Stoll, H.; Preuss, H. Theor Chim Acta 1990, 77, 123.

30. Schaefer, A.; Huber, C.; Ahlrichs, R. J Chem Phys 1994, 100, 5289.

31. Becke, A. D. Phys Rev A: At, Mol, Opt Phys 1988, 38, 3098.

32. Perdew, J. P.; Chevary, J. A.; Vosko, S. H.; Jackson, K. A.; Pederson, M. R.; Singh, D. J.; Fiolhais, C. Phys Rev B: Condens Matter 1992, 46, 6671.

33. Becke, A. D. J Chem Phys 1988, 88, 2547.

34. Mura, M. E.; Knowles, P. J. J Chem Phys 1996, 104, 9848; Murray, C. W.; Handy, N. C.; Laming, G. L. Mol Phys 1993, 78, 997.

35. Lebedev, V. I.; Laikov, D. N. Dokl Math 1999, 366, 741.

36. Elsässer, C.; Fähnle, M.; Chan, C. T.; Ho, K. M. Phys Rev B: Condens Matter 1994, 49, 13975.

37. Warren, R. W.; Dunlap, B. I. Chem Phys Lett 1996, 262, 384.

38. Fortunelli, A. J Mol Struct (Theochem) 1999, 493, 233.

39. Hoffmann, R.; Lipscomb, W. N. J Chem Phys 1962, 36, 2179.

40. Watari, N.; Ohnishi, S. J Chem Phys 1997, 106, 7531.

41. Fiorentini, V.; Methfessel, M.; Scheffler, M. Phys Rev Lett 1993, 71, 1051; 1998, 81, 2184.